Geotechnical Engineering Journal of the SEAGS & AGSSEA Vol. 42 No.3 September 2011 ISSN 0046-5828

Building Damage Assessment for Deep Excavations in Singapore and The Influence of Building Stiffness

K. H. Goh[1] and R. J. Mair[2]
[1]*Civil Design Division, Land Transport Authority, Singapore*
[2]*Engineering Department, University of Cambridge, Cambridge, UK*
E-mail: [1]kok_hun_goh@lta.gov.sg, [2]rjm50@cam.ac.uk

ABSTRACT: One of the biggest issues for underground construction in a densely built-up urban environment is the potentially adverse impact on buildings adjacent to deep excavations. In Singapore, a building damage assessment is usually carried out using a three-staged approach to assess the risk of damage caused by major underground construction projects. However, the tensile strains used for assessing the risk of building damage are often derived using deflection ratios and horizontal strains under 'greenfield' conditions. This ignores the effects of building stiffness and in many cases may be conservative. This paper presents some findings from a study on the response of buildings to deep excavations. Firstly, the paper discusses the settlement response of an actual building – the Singapore Art Museum – adjacent to a deep excavation. By comparing the monitored building settlement with the adjacent ground settlement markers, the influence of building stiffness in modifying the response to excavation-induced settlements is observed. Using the finite element method, a numerical study on the building response to movements induced by deep excavations found a consistent relationship between the building modification factor and a newly defined relative bending stiffness of the building. This relationship can be used as a design guidance to estimate the deflection ratio in a building from the greenfield condition. By comparing the case study results with the design guidance developed from finite element analysis, this paper presents some important characteristics of the influence of building stiffness on building damages for deep excavations.

1. INTRODUCTION

The continuing growth of population density in key urban centres around the world has placed greater emphasis on the development and utilisation of underground space to meet the demands of the city. Other than basement construction for building complexes for parking and other functions, many cities in the world are also embarking on major construction projects to put roads, metro systems, municipal services and utilities underground. To create this underground space, deep excavations are often made and these are supported using retaining walls with multiple props. Inevitably such excavations will cause movements of the ground behind the wall, particularly in soft ground conditions

To illustrate the ground movements that may arise during an excavation, a summary of deep excavation case histories in Singapore is tabulated in Appendix 1. The maximum wall deflection and the maximum surface settlement were normalised using the excavation depth, which can range from 7.5m to beyond 20m for metro basement excavation. By segregating the case histories into those involving excavation in soft clays and those involving excavation in stiffer soils, some differences in the ground movements can be identified. Firstly, as expected, excavations in soft clays cause more ground movements than excavations in stiff soils. The normalised wall deflection ranged from 0.24% to over 5% for excavations in the soft clays, and 0.11% to 0.45% for excavations in the stiffer soils, whilst the normalised maximum ground settlement ranged from 0.65% to over 4% in soft clays and from 0.09% to 0.21% in stiffer soils. This is consistent with the field observations summarised by Clough and O'Rourke (1990), where excavations in stiff soils caused settlements that are generally less than 0.3% times the excavation depth, whereas excavations in soft soils caused settlements that are more than 2% of the excavation depth. The case histories are also similar to the findings from Long (2001)'s extensive database of excavation case histories, where normalised maximum wall deflection in stiff clays is between 0.05%H and 0.25%H with normalized maximum vertical settlement values of up to 0.2%.

Furthermore, it is observed that the ratio between the maximum ground settlement and maximum wall deflection ranged from 0.38 to 0.82 in stiff soils. This is similar to the result obtained by Mana and Clough (1981) in their finite element analysis: the maximum ground settlement being 0.6 to 1.0 times the maximum wall deflection for an excavation in undrained conditions. However, for excavations in soft clay, the observed maximum ground settlement is often higher and can be more than twice that of the maximum wall deflection. This is likely attributed to consolidation-induced movements of the soft clays occurring during and after completion of the excavation (e.g. Nicholson, 1987).

2. BUILDING DAMAGE ASSESSMENT APPROACH AND INFLUENCE OF BUILDING STIFFNESS

The biggest impact of ground movements induced by underground construction is the potential effects on adjacent buildings and infrastructure. Typically, in the construction of major underground projects, hundreds of buildings could fall within the influence zone of the excavation and tunnelling activities. The challenge is to assess all of these buildings and structures, and identify those that might be adversely affected by the construction activities so that mitigation (and even possible remedial measures) can be recommended. To cope with such a large quantity of building assessments, an efficient approach is needed in order to do a first cut damage assessment for all buildings within the influence zone of the works. This will enable engineers to identify and select only the critical buildings for the subsequent, more rigorous and detailed assessment.

In Singapore, it is a requirement to do a building damage assessment during the design development of any major land transport infrastructure project (LTA design criteria, 2010). This is carried out using the three-staged approach outlined by Mair et al (1996) to assess the risk of building damage caused by such projects, as summarised in Figure 1.

In the preliminary assessment, the contours of excavation-induced settlements are drawn and buildings falling within a settlement zone of less than 10mm and having a slope of more than 1:500 are considered to have a negligible risk of damage and eliminated in this first stage. The remainder of the buildings is then subject to the second stage assessment using the limiting tensile strain method. This is done by calculating the maximum tensile strains induced in the building using deflection ratios and horizontal strains from simple beam theory, and then evaluating the maximum strains against the limiting tensile strains in order to estimate the potential damage category for each building. The approach assumes that the building has no stiffness and conforms to the greenfield displacement profile. Using the BRE classification system, summarised by Mair et al (1996), buildings assessed to have 'Negligible' damage, 'Very Slight' damage, and 'Slight' damage categories are considered to be at low risk of damage, and can be eliminated from the assessment at this stage. Finally, for buildings assessed to be at a high risk of damage (i.e. damage categories of 'Moderate', 'Severe' and 'Very Severe'), detailed evaluation is to be

undertaken. This could involve evaluating the structural details of the building, giving full consideration of the construction method in three-dimensions rather than plane-strain, as well as including soil-structure interaction effects which means taking into account the building stiffness. Following the detailed evaluation, consideration is then given to protective measures needed for buildings that remain in the high damage categories.

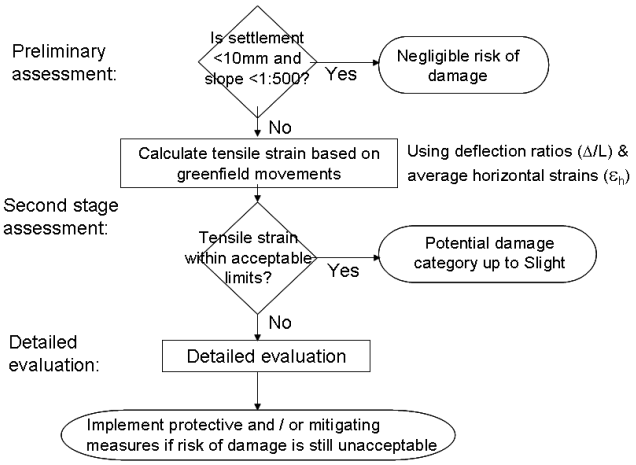

Figure 1 Building damage assessment using Mair et al (1996)'s staged assessment approach

During the second stage of building damage assessment, the tensile strains used for assessing the risk of building damage are derived using deflection ratios and horizontal strains under 'greenfield' conditions. This ignores the inherent stiffness of buildings and in many cases will be conservative. Potts and Addenbrooke (1997) proposed the building modification factor and relative stiffness approach to incorporate the influence of building stiffness for predicting building response to tunnelling-induced movements. Mair and Taylor (2001a, 2001b) used the approach of Potts and Addenbrooke to make Class A design predictions of building response (before the tunnelling) that were in good agreement with the monitored building response during the actual tunnelling works in London. Elshafie (2008) conducted centrifuge tests to study the effect of building stiffness on excavation-induced displacements. By subjecting buildings of various stiffnesses modelled using micro-concrete blocks to the effects of cantilever wall supported excavations, he found that increasing the stiffness of the building reduced the curvature of its settlement profile. However, at present there is very little guidance on how building stiffness can be accounted for when estimating building response to movements induced by deep excavations that are propped at several levels.

3. CASE STUDY OF THE SINGAPORE ART MUSEUM

Goh and Mair (2008) presented a new case study of the Singapore Art Museum to illustrate the influence of building stiffness on its response to excavation-induced movements. The Singapore Art Museum is a colonial-style building located in the heart of the historic civic district in Singapore. First constructed in 1867 as a school attached to a church, it consisted of a two-storey main building with east and west wings, and a chapel to the north with a separate building to the west. Over the period 1993-1996, the building was converted to the Singapore Art Museum through major alterations and additional works, which included the construction of new blocks and the reconstruction of several elements of the main building with its East and West wings. In the years 2002-2006, the main building was subjected to the effects of a deep excavation arising from construction of the Bras Basah MRT Station and the basement for the Singapore Management University. In particular, at the closest location, the excavation for the 35m deep Bras Basah Station was less than 7m from the wings of the main building. Figure 2 shows the site layout of the Singapore Art Museum and Figure 3 shows a cross-section of the deep excavation adjacent to the building.

A detailed instrumentation scheme was monitored in the vicinity of the Bras Basah Station construction and the Singapore Art Museum building (Osborne et al, 2005). In particular, precise levelling was used to monitor the settlement of markers on the building columns as well as on the non-suspended, tiled pavement just outside the building. This makes it possible to observe the influence of building stiffness on its response to excavation-induced settlements, by comparing the monitored building settlement with the adjacent ground settlement markers. Figure 4 shows the location of the building settlement and ground settlement markers, from which arrays of building settlement markers (SAM-1, SAM-2, SAM-4, SAM-5) may be compared with the corresponding arrays of ground settlement markers (BBS-1, BBS-2, BBS-4, BBS-5).

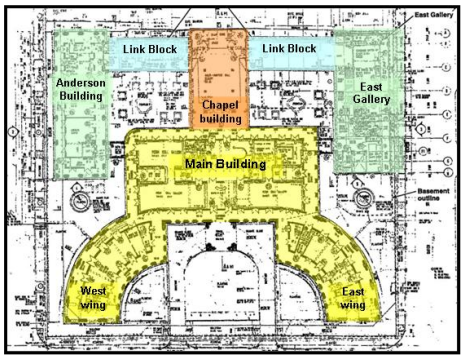

(a) Buildings of the Singapore Art Museum

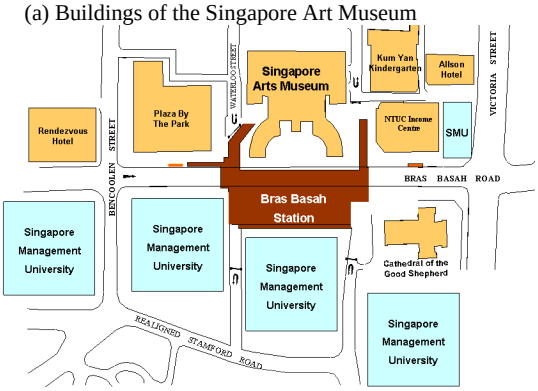

(b) Location of Singapore Art Museum and surroundings

Figure 2 Site layout of the Singapore Art Museum

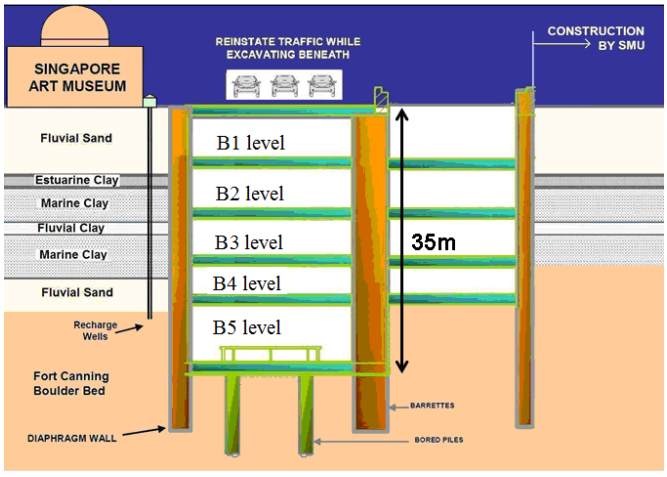

Figure 3 Schematic of Bras Basah Station (after Ong et al, 2006)

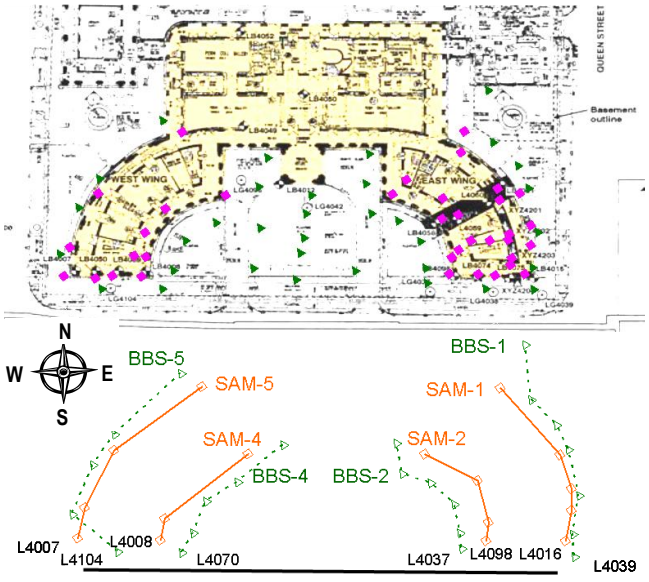

Figure 4 Location of building settlement (in squares) and ground settlement markers (in triangles)

Figure 5 shows the variation of settlement with time for selected ground and building settlement markers as well as key dates identified at various construction activities. As the case study is focused on excavation-induced movements, local effects of diaphragm walling works have been eliminated by setting the datum for all instruments to start from September 2003 onwards. To capture the full effects of consolidation movements, the timeline of the instrument readings ended around June 2006, which was more than one year after reaching the formation level of the Bras Basah excavation but by which the trends of settlement readings had suggested the end of the consolidation. Settlement response at intermediate periods has also been analysed to investigate the progressive response of the building. From Figure 5a, it may be seen that the ground settlement at the various array sections are different. The highest settlements occurred at the eastern-most ground settlement array at BBS-1, and these decrease towards the west wing of the main building. The big difference in ground settlement is due to the different amounts of consolidation-induced movements caused by the various excavation activities. This was pointed out by Osborne et al (2005), who noted that the maximum building settlement was higher than the maximum deflection of 25mm for the wall bordering the East wing of the museum building and found that the development of building settlement with time coincided with the periods of piezometric drawdown.

Figure 6 shows the ground and building settlement profiles at arrays BBS-1 and SAM-1 at various stages of the construction. These were at the easternmost section of the East Wing, and correspond to the location where the highest ground settlements were monitored. A maximum ground settlement of 92mm and a maximum building settlement of 68mm were observed for the period between September 2003 and June 2006. The ground settlement profile along array BBS-1 is in hogging mode behind the excavation during the early stages of excavation up to the roof level. As the excavation progressed, this changed to a sagging mode near the excavation and hogging mode away from the excavation. The point of inflexion which separates the building into sagging deformation and hogging deformation may be found by interrogating for the point of maximum slope on the settlement profile. Inspection of the settlement profiles indicates that there is a marked reduction in curvature of the building settlement profiles in building array SAM-1 compared to the ground settlement profiles in ground array BBS-1. The stiffer settlement response of the building can be attributed to its inherent stiffness.

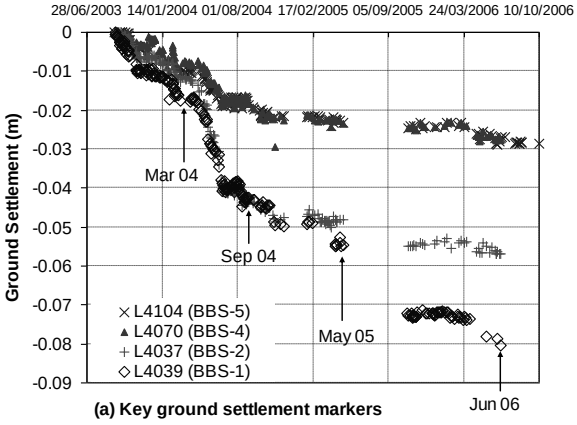

(a) Key ground settlement markers

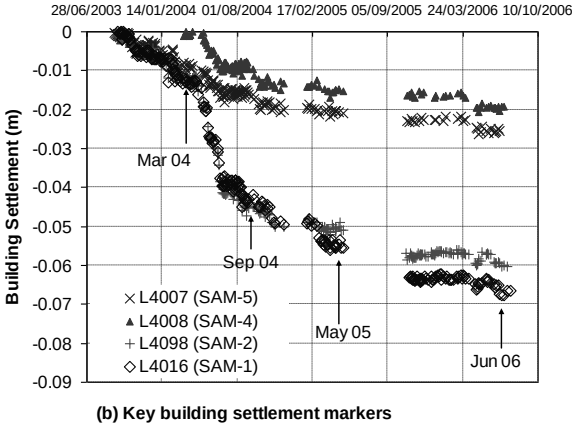

(b) Key building settlement markers

Timeline identified for analysis of Singapore Art Museum case study

Date	Key construction activity for Bras Basah Station
Sep 03	Start of Station excavation
Mar 04	Station excavation to roof level
Sep 04	Station excavated to B3 level
May 05	Station excavated to formation level at B5 level
Jun 06	1 year after B5 excavation completed

Figure 5 Variation of ground and building settlement with time (see Figure 3 for details of B3 and B5 levels)

Figure 7 shows the ground and building settlement profiles at arrays BBS-2 and SAM-2 at various stages of the construction. These settlement markers were located on the inner side of the East wing, and show a reduction from the location where maximum settlements were reported at arrays BBS-1 and SAM-1. The maximum ground and building settlement in this location is 59mm. The ground settlement profile is showing only sagging mode throughout the excavation period, and the building settlement profile shows less curvature than the ground settlement profile.

Figure 8 shows the ground and building settlement profiles at arrays BBS-4 and SAM-4 which are at the inner side of the West wing of the main building. The maximum settlement on the West wing reduced to about 30mm compared to the higher settlements at the East wing of the building. Furthermore, the ground settlement profile is almost linear at this location. The building settlement profile appears to give a sagging mode in some stages and a linear mode in others.

Figure 9 shows the ground and building settlement profiles at arrays BBS-5 and SAM-5 which are at the outside of the West wing of the main building. In contrast to the other sections, the settlement profiles for the ground and building are in hogging mode for all the excavation stages. Furthermore, the hogging deflection profiles for the building are quite similar to those for the ground. The building is very flexible in this section SAM-5 even though the structure is similar to the apparently stiffer section at array SAM-1 (see Figure 6).

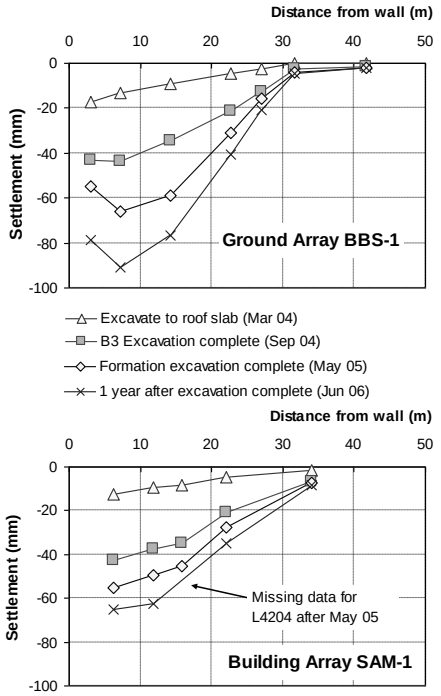

Figure 6 Settlement profiles for array BBS-1 and array SAM-1

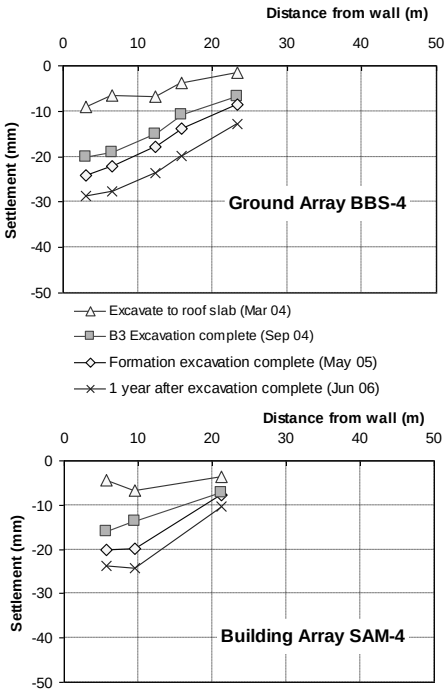

Figure 8 Settlement profiles for array BBS-4 and array SAM-4

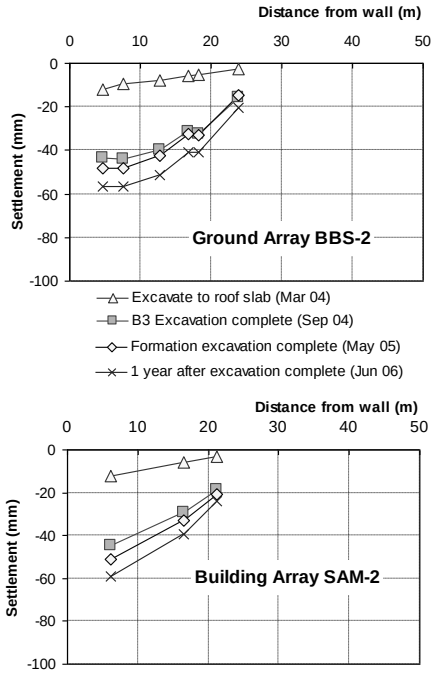

Figure 7 Settlement profiles for array BBS-2 and array SAM-2

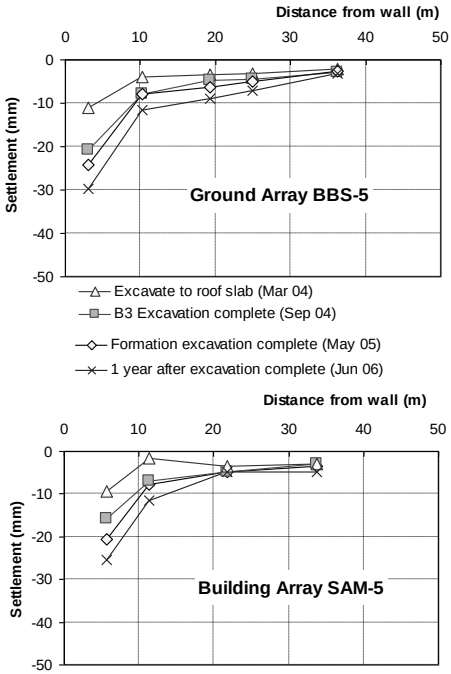

Figure 9 Settlement profiles for array BBS-5 and array SAM-5

The relative deflection (Δ) and the deflection ratios (Δ/L) in sagging and hogging zones were calculated at all the sections and corresponding to the various timelines, as shown in Table 1. To quantify the building's influence on the ground response, the building modification factor of deflection ratio – as defined by Potts and Addenbrooke (1997) – can be calculated by dividing the deflection ratio of the building by the corresponding deflection ratio of the adjacent ground (assumed to be the same as the greenfield condition). Figure 10 illustrates how the sagging and hogging lengths and relative deflections may be determined from the surface settlement curve induced during a deep excavation.

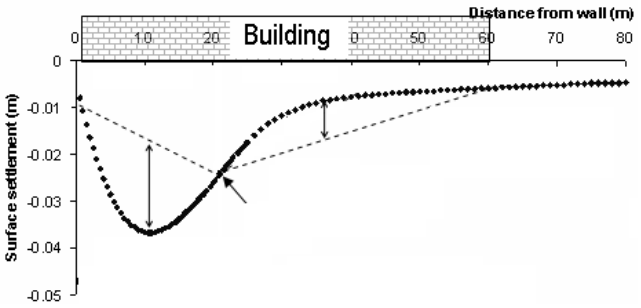

Figure 10 Determination of sagging and hogging lengths (L_{sag}, L_{hog}) and deflections (Δ_{sag}, Δ_{hog}) from surface settlement curve

Table 1. Relative deflection and deflection ratio in monitoring arrays

		Mar 2004 (exc. to roof)	Sep 2004 (exc. to B3)	May 2005 (exc. to B5)	Jun 2006 (one year after B5)
Ground array BBS-1	Max sag Δ	-	2.9mm	11.0mm	11.7mm
	Sagging L	-	20.8m	16.4m	16.4m
	Δ/L in sagging	-	0.0138%	0.0672%	0.0715%
	Max hog Δ	1.4mm	3.3mm	5.3mm	7.2mm
	Hogging L	27.8m	7.0m	11.4m	11.4m
	Δ/L in hogging	0.0049%	0.0478%	0.0467%	0.0637%
Building array SAM-1	Max sag Δ	-	5.2mm	6.5mm	8.5mm
	Δ/L in sagging	-	0.0333%	0.0410%	0.0537%
	Max hog Δ	1.9mm	-	-	-
	Δ/L in hogging	0.0069%	-	-	-
Ground array BBS-2	Max sag Δ	<1mm	4.8mm	5.0mm	6.2mm
	Sagging L	15.0m	15.0m	15.0m	15.0m
	Δ/L in sagging	0%	0.0317%	0.0334%	0.0415%
Building SAM-2	Max sag Δ	<1mm	2.7mm	2.8mm	4.4mm
	Δ/L in sagging	0%	0.0178%	0.0184%	0.0295%
arr ay 2	Max sag Δ	1.8mm	0.7mm	0.7mm	1.3mm
	Sagging L	15.6m	15.6m	15.6m	15.6m
	Δ/L in sagging	0.0118%	0.0044%	0.0042%	0.0081%
Building SAM-4	Max sag Δ	2.4mm	<1mm	2.8mm	3.7mm
	Δ/L in sagging	0.0154%	0%	0.0177%	0.0239%
Ground array BBS-5	Max hog Δ	3.5mm	5.9mm	7.7mm	7.6mm
	Hogging L	28m	28m	28m	28m
	Δ/L in hogging	0.0123%	0.0210%	0.0274%	0.0272%
Building SAM-5	Max hog Δ	6.4mm	6.2mm	9.4mm	9.8mm
	Δ/L in hogging	0.0230%	0.0221%	0.0337%	0.0352%

Due to the low deflection values in relation to the measurement errors of the surveying method (±1mm), the modification factors derived from an almost linear settlement profile would fluctuate substantially and not be meaningful. Hence, building modification factors were calculated only when the relative deflection of the ground was more than 3mm. As summarised in Table 2, the modification factors in sagging deflection are generally in the range of 0.55 to 0.75, whilst the modification factors in hogging deflection ranged from 1.05 to 1.29. These quantify the semi-rigid building response in sagging and the fully flexible building response in hogging that was observed in the settlement profiles.

Table 2. Building modification factors of deflection ratio

		Sep 2004	May 2005	Jun 2006
SAM-1	Sagging M^{DRsag}	-	0.61	0.75
SAM-2	Sagging M^{DRsag}	0.56	0.55	0.71
SAM-5	Hogging M^{DRhog}	1.05	1.23	1.29

4. DESIGN GUIDANCE TO INCLUDE THE INFLUENCE OF BUILDING STIFFNESS

To understand the influence of building stiffness, a numerical study of the response of buildings to ground movements induced by a deep excavation in soft clay was undertaken by Goh (2010) using finite element methods. The soft clay was modelled in Abaqus using the Modified Cam-Clay with properties that are similar to the Singapore Marine Clay, while the building was modelled as an elastic beam with bending stiffness and axial stiffness properties.

Figure 11 shows the variation of the building settlement and horizontal displacement profiles for buildings of various stiffnesses in one of the excavations modelled. For a flexible building with low bending stiffness, the building settlement behaviour is similar to that of the greenfield. As the bending stiffness increases, the settlement response becomes more rigid and the relative deflection decreases until the settlement trough becomes a straight line (when Δ=0). A building with a high bending stiffness will tend to tilt as a rigid body rather than distort under excavation-induced settlements. In terms of horizontal strains, a building with low axial stiffness will deform similar to the greenfield profile. As its axial stiffness increases, the horizontal strains in the building decrease until the response is so rigid that the entire building moves together with zero horizontal strains. Thus by realistically including the influence of building stiffness to estimate deflection ratios and horizontal strains, the

estimated maximum tensile strains induced in the building are reduced, resulting in a lower risk of building damage.

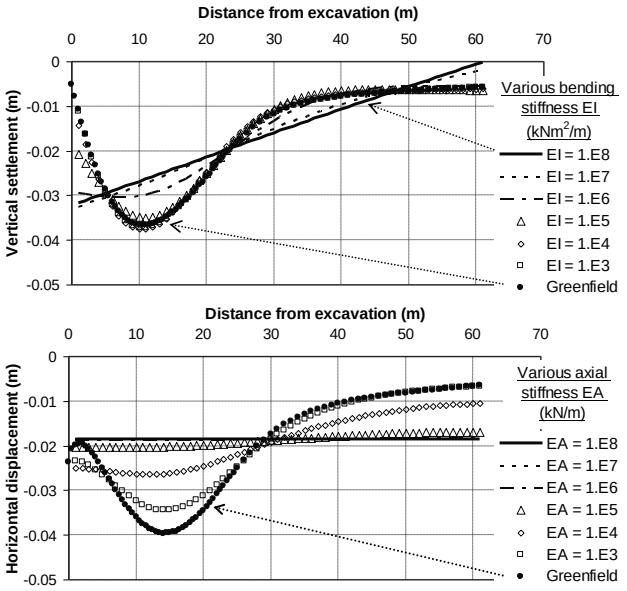

Figure 11 Settlement and horizontal displacement profiles for buildings of various stiffnesses

From the finite element study, it was found that there are several factors other than bending stiffness that would have an influence on building deformation behaviour. For example, a shorter building had a stiffer deflection response compared to a longer building with the same elastic stiffness in bending, and there is also an effect arising from the location of the building with respect to the excavation. Figure 12 shows the modification factors of the various building models for the same excavation configuration, where the building lengths and the building location are varied. For the same bending stiffness, there is a wide variation in the building modification factors due to different lengths and location.

A new measure of relative bending stiffness was then defined for buildings that were subjected to the influence of excavation-induced settlements. This relative bending stiffness ($\rho_{sag} = \frac{EI}{E_S * L_{sag}^3}$; $\rho_{hog} = \frac{EI}{E_S * L_{hog}^3}$) is dimensionless, and defined in terms of the elastic stiffness of the building (EI), divided by a representative soil stiffness (E_s), and divided by the cube of the sagging or hogging lengths in the greenfield condition corresponding to the building's location (L_{sag}; L_{hog}). The representative soil stiffness is defined as the weighted average of the elastic modulus of the soil above the excavation level, whilst the sagging and hogging lengths are estimated by identifying the inflexion point on the greenfield settlement profile. When the same modification factors in Figure 12 are plotted against the relative bending stiffness, the wide variation in the data points falls into a narrow cluster as shown in Figure 13. This shows that defining the relative bending stiffness in terms of the sagging and hogging lengths would be more generic compared to just using the bending stiffness of the building.

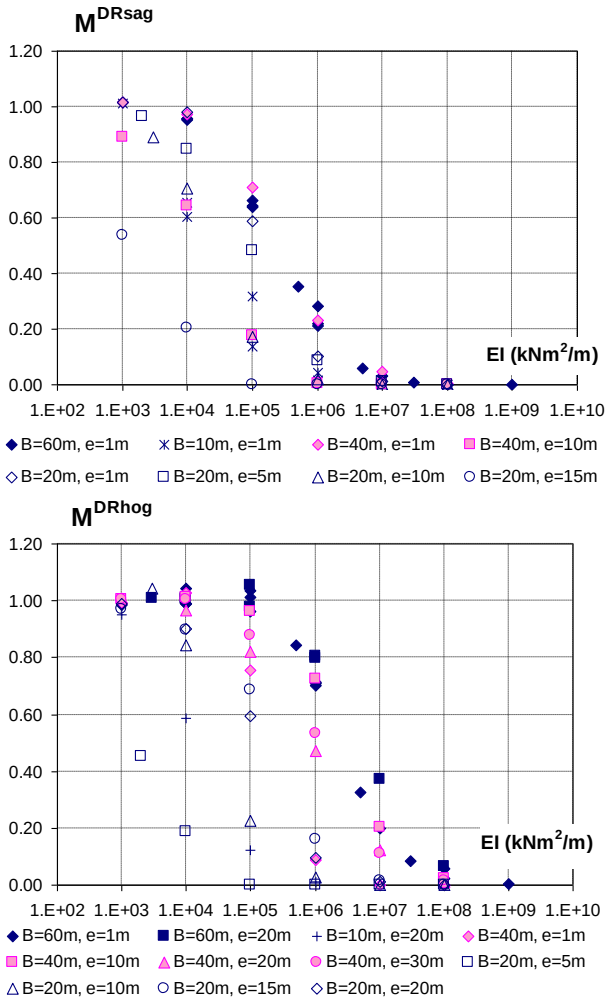

Figure 12 Deflection ratio modification factors (M^{DRsag}, M^{DRhog}) for buildings of various bending stiffness (EI) and at different lengths (B) and distances behind the excavation (e)

Furthermore, a series of parametric studies was conducted and it was found that the relationship between the building modification factor and the relative bending stiffness is fairly unique. The studies included varying the building lengths and building locations behind the excavation, changing various excavation characteristics such as depth of excavation, excavation support system, building weight, soil stiffness and constitutive model of the soil, composite soil profiles, and finally including the effects of consolidation. The full details and results are given in Goh (2010), but Figure 14 summarises the findings by showing that the building modification factors of deflection ratio for various finite element models fall into a close band when plotted against the relative bending stiffness of the building. When the relative bending stiffness is less than 10^{-4}, the modification factor is close to unity and the building would behave fully flexibly, having a deflection ratio similar to that of the greenfield. When the relative bending stiffness is more than 1, the modification factor is close to zero and the building would behave in a fully rigid manner, having zero deflection ratio. In between the two values, the modification factor decreases rapidly from unity to zero. As a result of the parametric studies, a design envelope may be drawn to describe the relationship between the building modification factors and the relative bending stiffness. This can be used to provide guidance on the influence of building stiffness on its settlement behaviour.

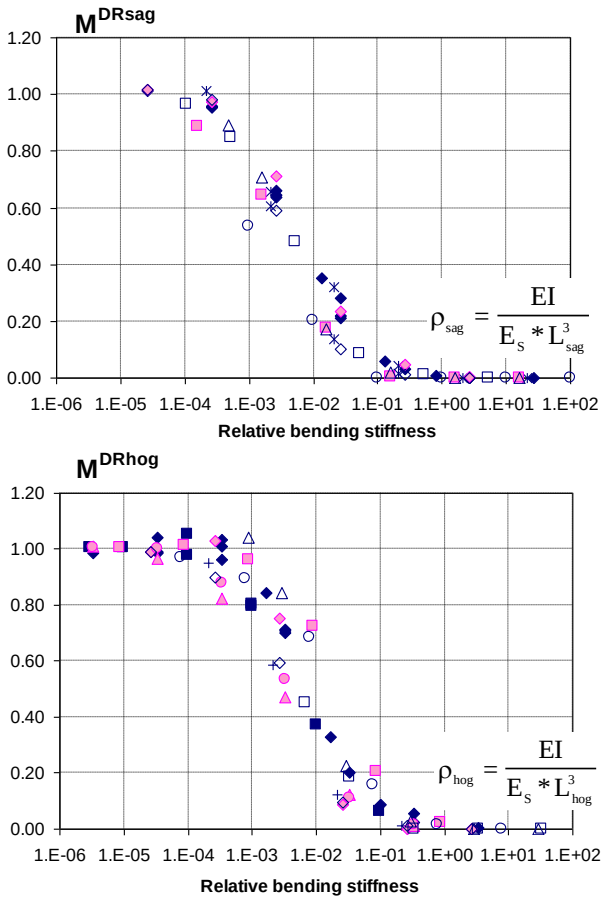

Figure 13 Deflection ratio modification factors (M^{DRsag}, M^{DRhog}) of buildings plotted against relative bending stiffness (ρ_{sag}, ρ_{hog})

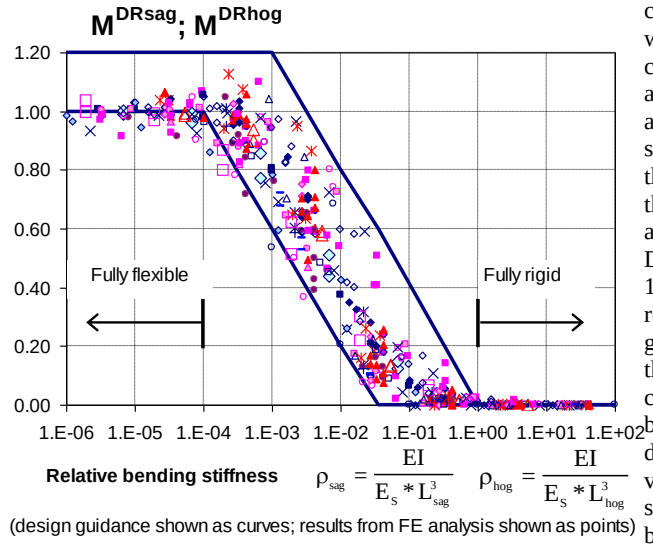

(design guidance shown as curves; results from FE analysis shown as points)

Figure 14 Proposed design guidance on modification factors of deflection ratio

5. COMPARISON OF FIELD STUDY WITH DESIGN GUIDANCE

A back-analysis of the Singapore Art Museum was then undertaken to compare the field observations with the design guidance developed from the numerical analysis. This was done by first estimating the bending stiffness of the building, and then comparing the observed deflection ratio modification factor with the modification factor plots developed using the finite element models.

(a) Front view of main building

(b) East Wing of main building

Figure 15 Masonry walls of the Singapore Art Museum

The structural behaviour of the Singapore Art Museum is dominated by the masonry walls that are of the original construction, as seen from the photographs in Figure 15. These walls were made of brick, rendered externally and in some locations covered with a variety of finishes. They were built as continuous arcades at the ground and first floors, and with average thickness of about 500mm. A trial pit showed that the walls have a relatively shallow foundation depth and are founded on timber layers above the water table – this was a common method of founding walls at that time. The roofs – also of the original construction – are pitched and covered with tiles, and are structurally supported using timber. During the massive addition and alteration works carried out in 1993-1996, the ground floor and the first floor of the building were reconstructed. Figure 16a shows the layout of the reconstructed ground floor together with the original columns in the East wing of the main building. The ground floor was based on a 125mm thick concrete slab, mesh reinforced with 300mm by 350mm downstand beams supported by micropiles. The micropiles comprise 75mm diameter driven steel tubes with a nominal capacity of 10 tons. They vary in length from about 20m to 30m. Figure 16b shows a cross-section view of the key structural elements supporting the main building. A separation membrane was installed so that the original masonry columns would not be structurally connected to the reconstructed ground floor slabs. Furthermore, most of the original slabs of the first floor were removed and replaced with 100mm thick concrete slabs on profiled metal permanent formwork. These are now supported on 350mm deep steel joists spanning between pockets cut into the original walls.

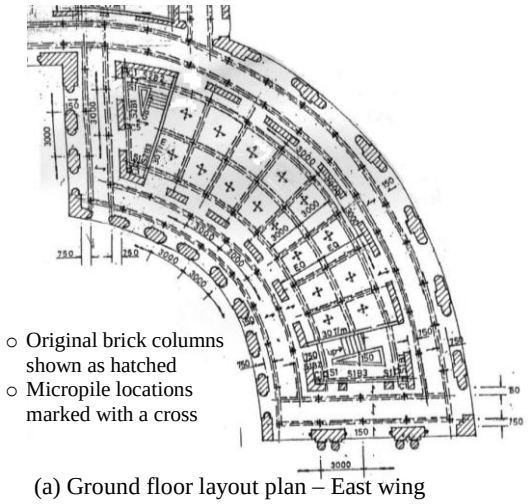

(a) Ground floor layout plan – East wing

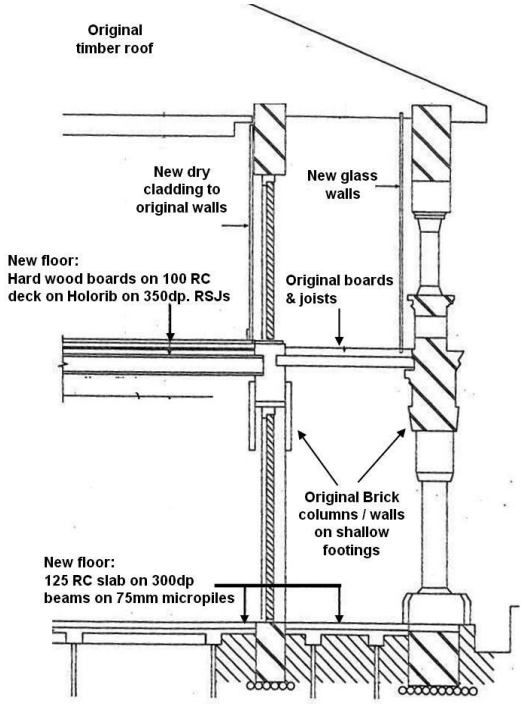

(b) Cross-sectional view

Figure 16 Key structural elements in the Singapore Art Museum

Appendix 2 shows how the relative bending stiffness of the Singapore Art Museum was estimated. The bending stiffness of the building is mostly due to the masonry walls as the floor slabs are thin and much more flexible in comparison. Without accounting for the effect of the wall openings, the bending stiffness of the Singapore Art Museum was estimated to be 5.07×10^7 kNm^2 per metre run. Using the weighted average of the elastic modulus of the soil above the excavation level of the Bras Basah Station, the representative soil stiffness was calculated and found to be around 47MPa. The different sagging and hogging lengths monitored in the ground settlement arrays were used to calculate the relative bending stiffness of the building at various sections, and this ranged from 0.24-0.32 at sagging arrays SAM-1 and SAM-2 to 0.048 at hogging array SAM-5. For the same building with similar ground conditions, there is a difference in the relative bending stiffness between the sagging and hogging deformation modes, by about an order of magnitude. This arises from the difference in the sagging and hogging lengths, resulting in a more flexible building for a longer hogging length and its semi-rigid response with a shorter sagging length.

Figure 17 plots the observed building modification factors against the estimated relative bending stiffness of the Singapore Art Museum, together with the design guidance developed from the finite element study. For the building modification factors inferred using field observations, the estimated relative bending stiffness is higher than what the finite element analysis would suggest, by about two orders of magnitude in sagging and about three orders of magnitude in hogging. The key reason for this difference is the large wall openings which had not been considered when making the bending stiffness estimate. A similar observation was made by Dimmock and Mair (2008), who had back-analysed the progressive tunnelling-induced deformation of the Moodkee Street houses in London for the Jubilee Line Extension project, and suggested that the wall openings had reduced the bending stiffness by an order of magnitude. Based on their field experience, Melis and Rodriguez Ortiz (2003) recommended a reduction factor to be applied on the bending stiffness of walls with various proportions of openings as shown in Table 3. From this case study, the wall openings seemed to have reduced the bending stiffness of the main building of the Singapore Art Museum by two orders of magnitude.

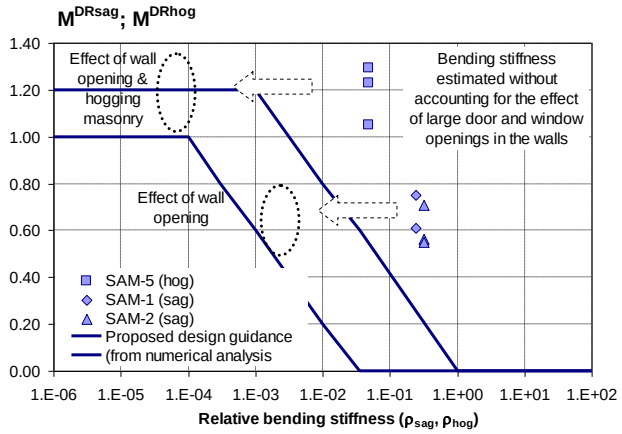

Figure 17 Modification factor plots of field study compared to numerical study

Table 3. Reduction factor on bending stiffness on walls (after Melis and Rodriguez Ortiz, 2003)

Type of wall	Length < H	Length > 2H
No openings	1.00	1.00
Openings from 0 to 15%	0.70	0.90
Openings from 15% to 25%	0.40	0.60
Openings from 25% to 40%	0.10	0.15
Openings more than 40%	0	0

Furthermore, even when the modification factors were plotted against the relative bending stiffness as shown in Figure 17, there is a discrepancy between the differences in the sagging and hogging deformation mode from the design guidance, by about an order of magnitude. This may be due to the different stiffness of masonry walls in sagging deformation and in hogging deformation. From their 3D finite element analysis of masonry facades under the influence of tunnelling-induced deformations, Burd et al (2000) observed that the facades subjected to sagging displacements were resistant to crack damage due to the lateral restraint provided by the ground, but those facades subjected to hogging mode of displacements are highly susceptible to crack damage with consequential loss of bending stiffness. Similarly, Dimmock and Mair (2008) had also observed that the bending stiffness of the masonry buildings at Moodkee Street in hogging deformation were lower than its bending stiffness in sagging deformation. These

studies suggest that the bending stiffness of masonry buildings may be different between sagging and hogging deformations.

6. CONCLUSIONS

Deep excavations can induce significant ground movements that may be detrimental to existing buildings, especially if the excavation is undertaken in soft clay. An efficient method to assess the impact of major excavation projects on existing buildings is to follow the three-staged approach of building damage assessment outlined by Mair et al (1996). However, during the second stage assessment, the limiting tensile strain method assumes the building has no stiffness and conforms to the greenfield deformations – in many cases this may be conservative.

In reality, the stiffness of a building would have an influence on its response to excavation-induced movements. This is observed in the case study of the Singapore Art Museum by comparing the monitored response of the building with the monitored response of the adjacent ground settlement markers. Specifically, the settlement response of the Singapore Art Museum was found to be semi-rigid in sagging and fully flexible in hogging, and this may be quantified using the building modification factor concept introduced by Potts and Addenbrooke (1997).

From the numerical studies described in this paper, it was observed that there are factors other than the bending stiffness of a building that affect its response to excavation-induced settlements, such as building length and its location on the settlement trough. However, by defining a new relative bending stiffness, a unique relationship between the building modification factors and the bending stiffness of the building was found. By subjecting this relationship to more rigorous parametric studies such as changing the excavation depths, excavation support system, soil profiles, etc., a design guidance has been proposed so that the building modification factors may be estimated from the relative bending stiffness of a building.

To illustrate the use of this design guidance, a back-analysis was made on the case study of the Singapore Art Museum, where the relative bending stiffness of the building was estimated for each monitored section of the building and then plotted against the building modification factor that was observed in the field. Due to its shorter sagging length, the relative bending stiffness of the building in sagging was lower than its relative bending stiffness in hogging. This explains the observed building settlement response being semi-rigid in sagging and more flexible in hogging. Furthermore, by comparing the field results with the design guidance developed from the finite element study, the influence of wall openings was found to reduce the bending stiffness of masonry walls at the Singapore Art Museum by at least two orders of magnitude – this is in agreement with findings by other researchers on the effects of wall openings on bending stiffness.

The design guidance developed from the finite element analysis is a useful tool to include the influence of building stiffness, so that a more realistic building response can be estimated and the reduction in deflection ratio from the greenfield condition can be assessed. Nevertheless, designers should also be aware that the estimate of the bending stiffness of actual buildings remains a challenge. In particular, for masonry structures, this should include the influence of wall openings and take account of differences in sagging and hogging deformation.

7. ACKNOWLEDGEMENTS

The authors would like to thank Mr. Nick Osborne for the information on the Singapore Art Museum. The first author would also like to thank the Land Transport Authority of Singapore for sponsoring his research study at the University of Cambridge.

8. REFERENCES

Burd, H. J., Houlsby, G. T., Augarde, C. E. and Liu, G. (2000). Modelling the effects on masonry buildings of tunnelling-induced settlement. Proc. Institution of the Civil Engineers, Geotechnical Engineering, Vol. 143(1), pp17–29.

Clough, G. W. and O'Rourke, T. D. (1990). Construction induced movements of in-situ walls. ASCE Geotechnical special publication No.25 – Design and Performance of Earth Retaining structures, pp 439–470.

Dimmock, P. S and Mair, R. J. (2008). Effect of building stiffness on tunnelling-induced ground movement. Tunnelling and Underground Space Technology, Vol. 23(4), pp.438–450.

Elshafie, M. Z. E. B. (2008). Effect of Building Stiffness on Excavation Induced Displacements. Ph.D. thesis, University of Cambridge, UK.

Goh, K. H. (2010). Response of Ground and Buildings to Deep Excavations and Tunnelling. Ph.D thesis, University of Cambridge, UK.

Goh, K. H. and Mair, R. J. (2008). Response of a building under excavation-induced ground movements. Proc. International Conference on Deep Excavations 2008, 10-12 Nov 2008, Singapore.

Long, M. M. (2001). Database for retaining wall and ground movements due to deep excavations. ASCE Journal of Geotechnical and Geoenvironmental Engineering, Vol. 127(3), pp 203–224.

Mair, R. J. and Taylor, R. N., (2001a). Elizabeth House: settlement predictions. In J.B. Burland, J.R. Standing, and F.M. Jardine (eds), Building Response to tunnelling – Case studies from construction of the Jubilee Line Extension, London. Vol. 1: Projects and Methods, pp.195–215, London: Thomas Telford.

Mair, R. J. and Taylor, R. N., (2001b). Settlement predictions for Neptune, Murdoch, and Clegg Houses and adjacent masonry walls. In J. B. Burland, J. R. Standing, and F. M. Jardine (eds), Building Response to tunnelling – Case studies from construction of the Jubilee Line Extension, London. Vol. 1: Projects and Methods, pp.217–228, London: Thomas Telford.

Mair, R. J., Taylor, R. N. and Burland, J. B., (1996). Prediction of ground movements and assessment of risk of building damage due to bored tunnelling, In R. J. Mair and R. N. Taylor (eds.), Proc. intern. symp. on Geotechnical Aspects of Underground Construction in Soft Ground, London, 15-17 April 1996, pp 713–718. Rotterdam: Balkema.

Mana, A. I. and Clough, A. M. (1981). Prediction of movements for braced cuts in clay. ASCE Journal of Geotechnical Engineering Division, Vol. 107(6), pp 759–777.

Melis, M. J. and Rodriguez Ortiz, J. M. (2003). Consideration of the stiffness of buildings in the estimation of subsidence damage by EPB tunnelling in the Madrid subway. In F. M. Jardine (ed.), Response of buildings to excavation induced ground movements, Proc. intern. conf., London, 17-18 July 2001, pp387–394, London: CIRIA.

Nicholson, D. P. (1987). The design and performance of the retaining walls at Newton Station. Proc. conf. Singapore Mass Rapid Transit Conference, Singapore, 6-9 April 1987, pp 147–154.

Ong, J. C. W., Osborne, N., Lim, H. T., Chang, K. B., Tew L. K., Chee, P., Johnson, P. and Lim, L. P., (2006). Bras Basah Station from a deep intricate excavation to a historic and landscape nucleus. Proc. International Conference on Deep Excavations, June 2006, Singapore.

Osborne, N. H., Ong, J. and Chang, K. B., (2005). Minimzing construction impact on a settlement sensitive building. Proc. conf. Underground Singapore 2005.

LTA design criteria (2010). Civil Design Criteria for Road and Rail Transit Systems (Rev A1, February 2010). Singapore: Land Transport Authority.

Potts, D. M. and Addenbrooke, T. I., (1997). A structure's influence on tunnelling-induced ground movements. Proc. Institution of the Civil Engineers, Geotechnical Engineering, Vol. 125(2), pp 109–125.

APPENDIX 1 – PUBLISHED CASE HISTORIES OF DEEP EXCAVATIONS IN SINGAPORE

Reference	Project	Max excavation depth (H)	Soil profile	Earth Retaining System	Normalised deflection – Max δw/H	Normalised settlement – Max Sv/H	Sv/ δw ratio
Tan et al (1985)	ENV Building	7.5m	1m Fill + 18m marine clay + 5m fluvial sand / clay above stiff clay	Sheetpile wall	5.33%	4.36%	0.82
Lee et al (1985)	CTC Building	11m	2m Fill + 21m marine clay + 7m fluvial clay + 6m soft clay above stiff clay	Sheetpile wall	1.71%	not available	not available
Nicholson (1987)	Newton Station	15m	2m Fill + 13m marine clay + 2m fluvial sand above stiff clay	0.8m thick D-wall	0.73%	1.33%	1.82
Hulme et al (1989)	Bugis Station	18m	4m Fill + 28m marine clay + 2m fluvial sand above stiff clay	1.2m thick D-wall	0.83%	1.11%	1.33
Wallace et al (1993)	UOB Building	13m	3m Fill + 17m marine clay + 2m fluvial clay + 11m marine clay above stiff clay	1.2m thick D-wall	0.42%	0.96%	2.27
Lee et al (1998)	IMM Building	17m	2m Fill + 15m marine clay + 11m fluvial sand / clay above stiff clay	1m thick D-wall	0.62%	0.68%	1.10
Raju et al (2000)	Clarke Quay Station	22m	2m Fill + 22m marine clay above stiff clay	1.2m thick D-wall	0.48%	0.64%	1.33
Orihara et al (2001)	Dhoby Ghaut (Section D)	11m	2m Fill + 8m marine clay + 2m fluvial sand above stiff clay	ϕ1m secant pile wall	0.77%	0.82%	1.06
Wen et al (2001)	Race Course Road tunnel	17m	4m Fill + 5m fluvial sand + 13m marine clay above stiff soil	0.8m thick D-wall	0.24%	0.65%	2.75
Chandra et al (2006)	The Sail @ Marina Bay	8.5m	5m fill + 27m marine clay + 3m fluvial deposits above stiff clay	Multi-cell D-wall + cross-wall	0.12%	0.18%	0.67
Chua et al (2008)	Pasir Panjang Station	20m	3m fill + 17m marine clay / fluvial deposits above stiff clay	1m thick D-wall + cross-wall	0.08%	not available	not available
Ng and Fun (2010)	New Nicoll Highway Station	20m	7m fill + 24m marine clay + 3m fluvial sand + 10m marine clay + 3m fluvial sand above stiff clay	1.5m thick D-wall + ground improvement	0.10%	not available	not available
Leonard et al (1987)	Tiong Bahru Station	15m	Jurong Formation	Soldier pile wall	0.17%	not available	not available
Leonard et al (1987)	Somerset Station	15m	Residual soils	0.6m thick D-wall	0.13%	not available	not available
Kong et al (2000)	Tan Tock Seng Hospital	16.5m	Jurong Formation	Contiguous bored piles	0.45%	0.21%	0.48
Jeyatharan and Song (2000)	Kovan Station	18m	Old Alluvium	0.6m thick D-wall	0.11%	0.09%	0.82
Lee at al (2001)	Woodleigh, Serangoon	25m	Residual soils	Soldier pile wall	0.40%	0.15%	0.38

References for Excavation Case Studies in Singapore

Chandrasegaran,S., Gilbert, C., Jeanmaire, T., Nasim, S.Quereshi.J., Lauw S.W, Tan S.A., Perez, F., Calimag, F., and Furio, R. (2006.) Triple cellular diaphragm wall in Singapore marine clay, *Proc. Of International Conference on Deep Excavations 28-30 June 2006, Singapore.*

Chua, T. S.,Lew. M., Rama, V., and Phua, H. L. (2008). Robust Earth Retaining Wall System to Control Ground Movement andMinimize Impact on Adjacent Structures, *Proc. Of International Conference on Deep Excavations, 10- 12 Nov 2008, Singapore*.

Hulme, T. W., Potter, L.A.C. and Shirlaw, J.N. (1989). Singapore MRT System: Construction. *Proc. Inst Civil Engineers,* 86: pp709–770.

Kong, S. K., Yang, D. Q. and Lai, K. S. (2000). Behaviour and performance of deep excavation in residual soils near sensitive structures. In J. Zhao, J.N. Shirlaw & R. Krishnan (eds.), *Tunnels and Underground Structures, Proc. intern. conf*: pp457-463, Rotterdam: Balkema.

Jeyatharan, K. and Song, T. W. (2000). Some observations during excavation on the behavior of old alluvium soils in Singapore In J. Zhao, J. N. Shirlaw & R. Krishnan (eds.), *Tunnels and Underground Structures, Proc. intern. conf., Singapore, November 2000*: pp413-420, Rotterdam: Balkema.

Lee, S. L., Karunaratne, G. P., Lo, K. W., Yong, K. Y. and Choa, V. (1985). Developments in soft ground engineering in Singapore. *Proc. of the 11th International Conference on Soil Mechanics and Foundation Engineering, San Francisco, 12-16 Aug 1985,* 3: pp1661–1666

Lee, F. H., Yong, K. Y., Quan, K.C.N. and Chee, K. T. (1998). Effects of corners on strutted excavations: Field monitoring and case histories. *ASCE Journal of Geotechnical and Geoenviromental Engineering* 124(4): pp339–349.

Lee, F. H., Tan, T. S. and Wang, X. N. (2001). Groundwater effects in soldier-piled excavations in residual soils. *Proc. conf. Underground Singapore 2001*: pp249–260.

Leonard, M.S., Wong, H. and de Labrusse, P. (1987). The design and performance of temporary works for Somerset and Tiong Bahru stations. *Proc. conf. Singapore Mass Rapid Transit Conference, Singapore, 6-9 April 1987*: pp141–145.

Nicholson, D.P. (1987). The design and performance of the retaining walls at Newton Station. *Proc. conf. Singapore Mass Rapid Transit Conference, Singapore, 6-9 April 1987*: pp147–154.

Ng, C.C. and Fun, W.S. (2010). Challenges in Design & Construction of New Nicoll Highway Station and Tunnels after the Collapse. *Proc. of the World Urban Transit Conference 2010, Singapore*: pp101-109.

Orihara, K., Chan, M.L., Chabayashi, K., Okamoto, S., Teo, P.T.P .and Tan, C.G. (2001). Excavation of new Dhoby Ghaut station for MRT North-East Line. *Proc. conf. Underground Singapore 2001*: pp183–192.

Raju, G.V.R., Lim, K. and Endicott, J. (2000). Geotechnical design and construction aspects of the Clarke Quay station. In J. Zhao, J.N. Shirlaw & R. Krishnan (eds.), *Tunnels and Underground Structures, Proc. intern. conf*: pp405-412, Rotterdam: Balkema.

Tan, S.B., Tan, S.L. and Chin, Y.K. (1985). A braced sheetpile excavation in soft Singapore marine clay. *Proc. of the 11th International Conference on Soil Mechanics and Foundation Engineering, San Francisco, 12-16 Aug 1985*, 3: pp1671–1674.

Wallace, J.C., Ho, C.E. and Long, M.M. (1993). Retaining wall behaviour for a deep basement in Singapore marine clay . *Proc. ICE conference on retaining structures, July 1992, Cambridge*: pp195-204, London: Thomas Telford.

Wen, D., Ow, C.N. and Yoon, S.I. (2001). The monitoring of cut and cover tunnel construction at Race Course Road next to Foochow Methodist Church. *Proc. conf Underground Singapore 2001*: pp 261–271.

APPENDIX 2-ESTIMATING RELATIVE BENDING STIFFNESS OF SINGAPORE ART MUSEUM

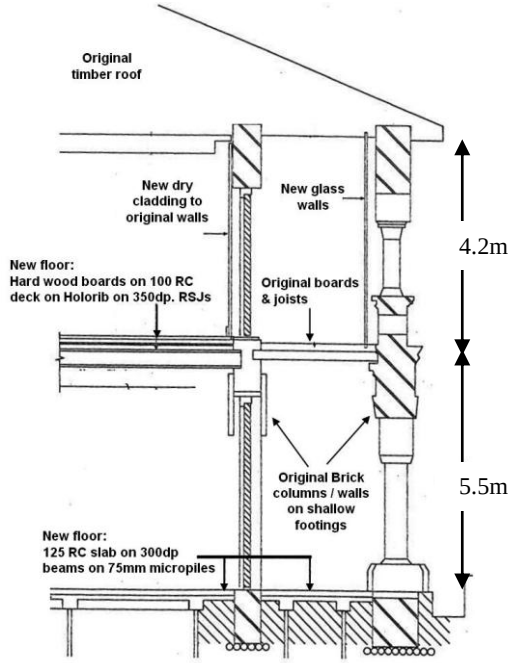

Bending stiffness of building EI

- Masonry walls (up to 750mm thick, and with large openings)
  Assume 500mm thick on average, with wall height of 4.2+5.5 = 9.7m
  For each 500mm thick masonry wall, EI = $5x10^6$ * [9.7^3*0.5 / 12] = 1.9 x 10^8 kNm^2 per wall. Since there are 4 walls on each wing (over a 15m length of the building), bending stiffness of the masonry walls = 1.9 x 10^8 * (4 / 15) = $5.07x10^7$ kNm^2 per metre run.
- Bending stiffness of 100mm thick RC slab at first floor = $23x10^6$ * [0.1^3 / 12] = 1917 kNm^2 per metre run
- Bending stiffness of 1mm thick Holorib steel formwork at first floor = $205x10^6$ * [$0.001*0.05^2$] = 513 kNm^2 per metre run
- 125mm thick RC slab at ground floor does not contribute to bending stiffness due to independent structure.
- Structural elements parallel to excavation do not contribute to bending stiffness – thus no contribution from the 350mm deep rolled steel joists.

Hence, without accounting for reduction of stiffness due to large openings, total bending stiffness of building, EI = ($5.07x10^7$ + 1917 +513) = $5.07x10^7$ kNm^2 per metre run.

Representative soil stiffness Es

The borelogs M3019 and M3005 are used to define the soil stratigraphy at the East Wing and the West Wing of the museum building respectively. The representative soil stiffness is defined as the weighted average of the elastic stiffness for all the soil layers above the excavation level. For the 35m deep excavation, the representative soil stiffness for the East Wing and West Wing soil profiles are as estimated :-

- At East Wing

  Soil profile above excavation level consists of 1m Fill, 8m Fluvial sand, 4m Marine Clay, 6m Fluvial sand, and 16m of Fort Canning Boulder Bed.

Using the weighted average method, the undrained modulus of soil above final formation level

Eu = (1*10+8*20+4*3.3+6*20+16*100) / 35 =54MPa (1)

Since $E' = \frac{1+\upsilon'}{1+\upsilon_u} * Eu$, the representative soil stiffness

Es = 1.3/1.5*54 = 47MPa.

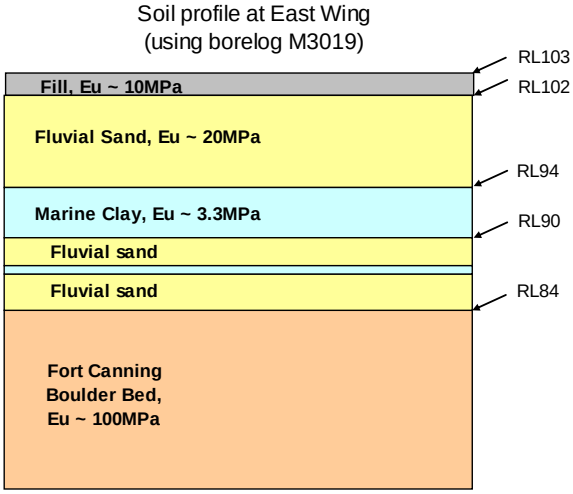

- At West Wing

  Soil profile above excavation level consists of 1m Fill, 7m Fluvial sand, 5m Fluvial clay, 2m Marine Clay, 4m fluvial sand, and 16m of Fort Canning Boulder Bed.

Using the weighted average method, the undrained modulus of soil above final formation level

Eu = (1*10+7*20+5*20+2*4.2+4*20+16*100) / 35 =55MPa (2)

Since $E' = \frac{1+\upsilon'}{1+\upsilon_u} * Eu$, the representative soil stiffness

Es = 1.3/1.5*55 = 48MPa.

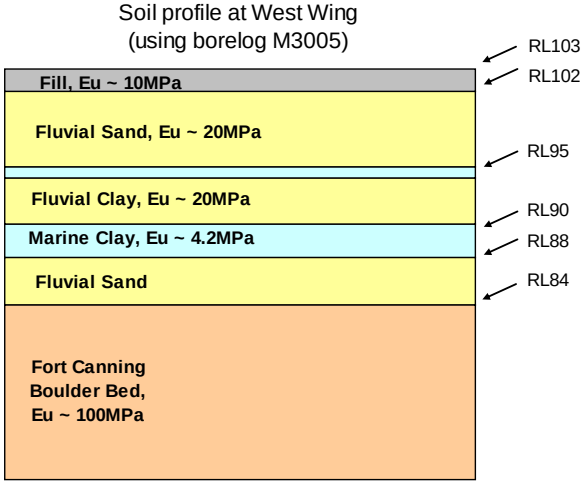

Relative bending stiffness, ρ_{sag} and ρ_{hog}

To calculate the relative bending stiffness at various building sections,

- At array BBS-1, ground sagging length, L_{sag} = 16.4m
  Thus, relative bending stiffness at
  SAM-1, $\rho_{sag} = EI/Es/L_{sag}^3 = 5.07x10^7 / 47x10^3 / 16.4^3 = 0.24$.

- At array BBS-2, ground sagging length, L_{sag} = 15.0m
  Thus, relative bending stiffness at
  SAM-2, $\rho_{sag} = EI/Es/L_{sag}^3 = 5.07x10^7 / 47x10^3 / 15.0^3 = 0.32$.

- At array BBS-5, ground hogging length, L_{hog} = 28.0m
  Thus, relative bending stiffness at
  SAM-5, $\rho_{hog} = EI/Es/L_{hog}^3 = 5.07x107 / 48x103 / 28.03 = 0.048$.